# Self-Diffusion and Cooperative Diffusion of a Rodlike DNA Fragment

**Lixiao Wang,† Mark M. Garner,‡ and Hyuk Yu***

*Department of Chemistry, University of Wisconsin, Madison, Wisconsin 53706*

*Received March 26, 1990; Revised Manuscript Received November 27, 1990*

ABSTRACT: The self-diffusion and cooperative diffusion of a 150 base pair DNA fragment have been studied as a function of DNA concentration at three different salt concentrations (in the range of 1 mM to 1 M NaCl) in semidilute solution. In the 1 mM NaCl concentration, slow and fast relaxation modes were observed by quasi-elastic light scattering while only one relaxation mode was observed by forced Rayleigh scattering. The slow mode is shown to be not a self-diffusion process. In the high-salt conditions, the dynamics of rodlike DNA were discussed in the context of Doi and Edwards theory. The experimental results in low-salt conditions are compared with the scaling theory and the coupled-mode ion diffusion theory of Lin, Lee, and Schurr.

## Introduction

Since the work of Doi and Edwards[1] on the dynamics of rigid-rod and wormlike macromolecules in semidilute and concentrated solutions, Fixman[2] has criticized the cage notion by simulation studies and Doi et al.[3] have derived the cooperative diffusion coefficient in the isotropic phase. At the same time, dynamics of charged polyelectrolytes in such solutions have been extensively studied theoretically[4,5] and experimentally.[6-17] The dynamics of charged rodlike macromolecules are of great interest, in part because they constitute an important class of biological systems. Moreover, transport phenomena of the biological systems in general are clearly of interest in terms of their relationship to the biological functions.

Dynamics of short, rodlike DNA fragments are complicated since the solution can exist in at least four different states,[14] a liquid crystal at high DNA concentration, a clear viscoelastic gel at moderate DNA concentration, an "extraordinary phase" with a very slow translational diffusion in low salt, and an isotropic fluid at low DNA concentration. Transitions among these states depend strongly on salt concentration, DNA concentration, molecular weight, and temperature. Ionic strength effects on the cooperative diffusion of these fragments have been studied by quasi-elastic light scattering (QELS), whereby two exponential decay modes, fast and slow, have been found. On the other hand, a self-diffusion coefficient has not yet been reported in the literature. Furthermore, the strong and complex salt dependence found in the QELS studies points to potential difficulties in extracting structural information of polyions at low ionic strength from such studies.[14]

The objective of this paper is to further our understanding of the "ordinary-extraordinary transition" by self-diffusion studies and to examine the DNA concentration dependence of the self-diffusion and cooperative diffusion coefficients in dilute and semidilute concentration regimes. In addition, we attempt to relate the dependence of the cooperative diffusion and self-diffusion coefficients on DNA concentrations to chain interaction in low-salt and high-salt conditions by interpreting our results in the context of the current theoretical predictions. The forced Rayleigh scattering (FRS) technique was used to obtain self-diffusion coefficients $D_s$ and the QELS technique to obtain the slow and fast cooperative diffusion coefficients $D_c$, so that $D_s$ could be directly compared with $D_c$ under the same conditions. We should note here that Nicolai and Mandel[6] have already reported their dynamic and static light scattering results for the same system and our $D_c$ results are on the whole in agreement with theirs, while we add to what are known to date with our self-diffusion studies.

## Experimental Section

**Materials.** DNA was isolated from fresh chicken blood, following the procedure of Shindo et al.[18] The procedure starts with the isolation of chicken erythrocyte nuclei from the fresh blood of an adult rooster. The isolated nuclei were digested with 50 units/mL micrococcal nuclease (Worthington) at 37 °C for 30 min and then lysed by dialysis as described.[18] After precipitation of the H1/H5 containing chromatin, the nucleosome core particles were treated with proteinase K, phenol/chloroform was extracted, and the resulting DNA ethanol was precipitated. The measured UV absorbance ratios, $A_{260}/A_{280}$ and $A_{260}/A_{230}$, were 1.87 and 2.12, respectively, indicating an essentially protein-free DNA sample. The purity of this DNA was assayed by electrophoresis on 7% polyacrylamide gels and found to consist of approximately equal amounts of 140 and 160 base pair (bp) in length, similar to that by Fulmer et al.[15] The composition is further examined before and after 4 months of experimental period, whereby we have confirmed that the DNA has not undergone any denaturation during the course of the experiment.

Two chemicals used for DNA labeling, 4-fluoro-3-nitrophenyl azide and 4-(*N*,*N*-dimethylamino)azobenzene 4′-isothiocyanate, were purchased from Pierce Chemical Co. (Rockford, IL), *N*-(3-aminopropyl)-*N*-methyl-1,3-propanediamine, a spacer moiety (see below), was from Tokyo Kasei, and 1,4-bis(3-aminopropyl)-piperazine was from Aldrich Chemical Co. (Milwaukee, WI). All four were used as received without further purification.

**Labeling of DNA.** The labeling procedure is similar to the biotinylation of DNA by Forster et al.[19] The procedure starts with preparation of an appropriate dye with a spacer linkage connecting the azide group at one end and the azobenzene group at the other end. Upon brief irradiation with visible light, the azide groups were subsequently reacted with double-stranded nucleic acids to complete the labeling procedure. The chemistry of the labeling is schematically shown in Scheme I. Detailed procedures are as follows.

**(a) Dye Preparation.** All reactions involving the formation and use of aryl azides were carried out in the dark. A solution of 4-fluoro-3-nitrophenyl azide (0.68 g, 3.73 mmol) in dry ether (8 mL) was added with stirring to a solution of *N*-(3-aminopropyl)-*N*-methyl-1,3-propanediamine or 1,4-bis(3-aminopropyl)piperazine (3.2 mL) in dry ether (20 mL), and the mixture was stirred for 45 min. The resulting red product was subsequently dissolved in water (25 mL). The solution was made basic by adding 25 mL of 1 M NaOH, and the product was extracted into ethyl acetate

† Present address: Department of Biochemistry, College of Biological Science, University of Minnesota, St. Paul, MN 55108.
‡ Present address: Max-Plank-Institut für biophysikalische Chemie, Am Fassberg, 3400 Göttingen, FRG.

0024-9297/91/2224-2368$02.50/0 

**Scheme I**
**DNA Modification and Labeling Procedure**

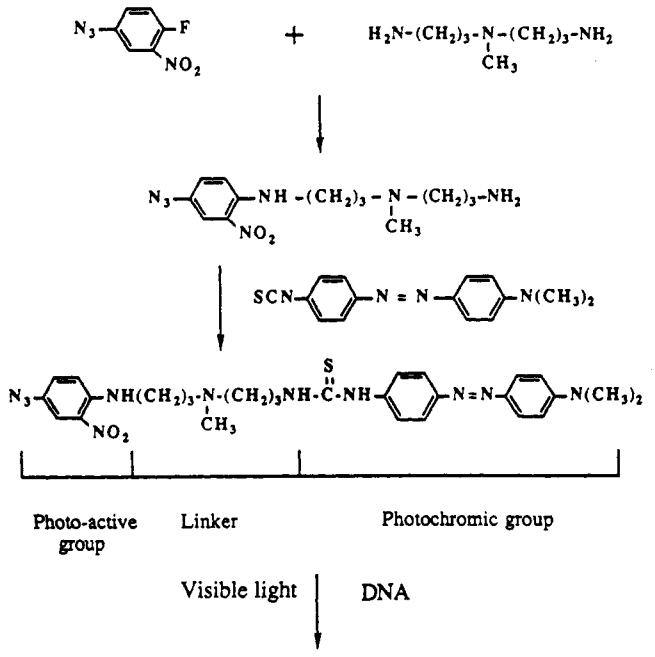


(3 × 50 mL). The pooled ethyl acetate extracts were dried over $Na_2SO_4$; subsequently the solvent was removed to give the crude product, which was dissolved in 60 mL of tetrahydrofuran. A sample of the tetrahydrofuran solution (20 mL) of the above product was allowed to react with 0.43 g (1.52 mmol) of 4-(*N*,*N*-dimethylamino)azobenzene 4′-isothiocyanate in 25 mL of dry tetrahydrofuran at room temperature for 1 day. The reaction mixture was used for the subsequent step without further purification.

**(b) Dye Labeling of DNA.** Under very subdued light, 2 mL of the above reacted mixture was added in 20 mL of deionized water; then tetrahydrofuran was removed. The aqueous dye solution was added in 40 mL of DNA solution (0.625 g/L), which was dialyzed in deionized water (pH = 7) for 10 h at 4 °C. The solution was cooled in an ice–water bath 10 cm below a sunlamp (275 W) and irradiated for 30 min. Because of enormous heat produced by the sunlamp, the bath temperature was checked every 5 min to maintain low temperature (1 °C). At the beginning of the irradiation, gas bubbles (presumably those of nitrogen) appeared within the solution. The red solution was then added to 0.1 M Tris-HCl, pH = 9 (40 mL), its volume was increased to 150 mL with water, and the solution was extracted repeatedly with *n*-butanol (100 mL) until no unreacted dye was visually observed in the butanol layer. The volume of the red aqueous phase was increased with 0.4 M sodium acetate to 100 mL; then cold ethanol (250 mL) was added, and the dye-labeled DNA was precipitated at −20 °C overnight. Centrifugation (4 °C, 30 min) yielded a red pellet. The pellet was dried and dissolved in 0.1 mM EDTA. The labeled and unlabeled DNA samples were run in parallel on 7% polyacrylamide gels, and the mobility of both samples was found to be identical, indicating the labeling procedure did not denature the DNA sample. The dye content of labeled DNA was determined spectrophotometrically, and it was found that the labeling yield was about 0.75 dye/DNA fragment. The absorbance at 460 nm was used to determine the dye content of the labeled DNA.

**Preparation of DNA Samples for Measurements.** All solutions were prepared with deionized water, which was prepared from house distilled water upon passing through the Millipore Q2 system (Millipore) with one carbon and two ion-exchange filters, and NaCl of analytical grade (Merck). They were made dust free by filtration through 0.2-μm Acrodisc filters. Mononucleosomal DNA solutions were exhaustively dialyzed (4 × 500 mL over a period of 24 h) at 4 °C against buffer solutions of various ionic strengths. DNA concentrations were determined

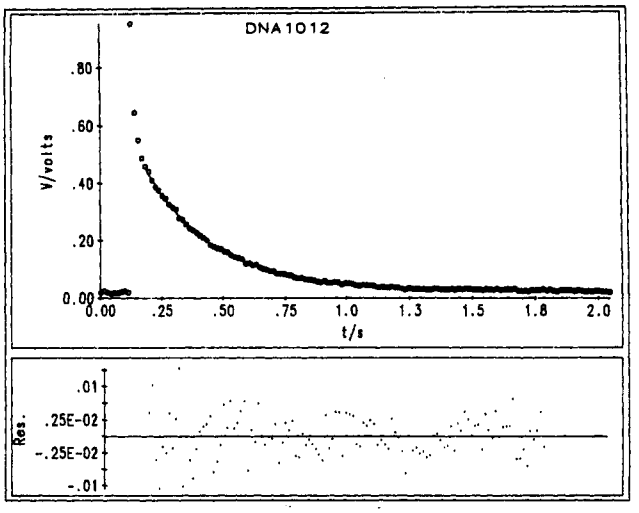


**Figure 1.** Rise and decay profile of the diffracted reading beam intensity. The top portion of this figure shows the average value of the photomultiplier output from six transients plotted as $V(t)$ in volts vs time in seconds for a DNA, 150 bp, at 6.5 g/L, 1 mM NaCl, 20 °C and at an angle of 59.22 mrad. The background signal for a few pretrigger time intervals is included to emphasize the return of the signal to the base line. The best fit curve to the decay profile using the model function as described in the text is drawn through the data in the upper graph, while the normalized residuals from that fit on the identical time scale are shown in the bottom graph, indicating a good fit to the data by their random distribution.

by optical absorption at 260 nm by using the extinction coefficient of 20 $mg^{-1}$ mL $cm^{-1}$. Buffers used in this experiment were 2.5 mM Tris and 0.1 mM EDTA, pH 8.95 at 20 °C. The samples so prepared were diluted to various DNA concentrations with the same buffer used in the dialysis experiments.

**Methods.** The optical configuration of the FRS instrument, the data acquisition, and the analysis scheme is the same as that in our previous work[20] from this laboratory. All the experiments were performed at 20.0 ± 0.2 °C. The decay profiles can be fit with a single-exponential model function by using the typical relation[21]

$$V(t) = (Ae^{-t/\tau} + B)^2 + C^2 \quad (1)$$

where $V(t)$ is the photomultiplier output of the FRS signal, $A$ is the preexponential amplitude of the diffracted optical field, $B$ is the coherent scattering background of the optical field, $\tau$ is the relaxation time of the diffracted optical field, and $C^2$ is the background intensity from incoherent scattering and stray light. The four parameters are determined by a nonlinear least-squares fitting routine on a Vax 8600 computer. A typical FRS signal, the rise and decay of the diffracted light intensity, and the best fit according to eq 1 are displayed in Figure 1. The small root-mean-square residuals and its random distribution demonstrate a good fit to the model function. In any case, the final criterion to accept a given set of measurements is the reproducibility of the decay profiles and the confirmation of the decay time constant ($\tau^{-1}$) dependence on the scattering wave vector $q$, $\tau^{-1} \propto q^2$. Having obtained the values of $\tau$ over more than five different angles, we determined the diffusion coefficient from the slope of a least-squares fit according to the relation[22]

$$1/\tau = 1/\tau_{life} + D_s q^2 \quad (2)$$

Here, $\tau$ is the measured decay time constant of the FRS signal, $\tau_{life}$ is the lifetime of the photochromically shifted state of the dye, and $D_s$ is the self-diffusion coefficient. The $q^2$ dependence of the decay time constant of the FRS signal is displayed in Figure 2. These set of data are obtained from labeled 150 ± 10 bp DNA in 0.2 M NaCl concentration with three DNA concentrations. As DNA concentration increases, the plot shows a gradual decrease of the self-diffusion coefficients, which is represented as the slope of the plot according to eq 2.

The instrument used for QELS was the same one as that in the report by Amis et al.[23] The quasi-elastic light scattering

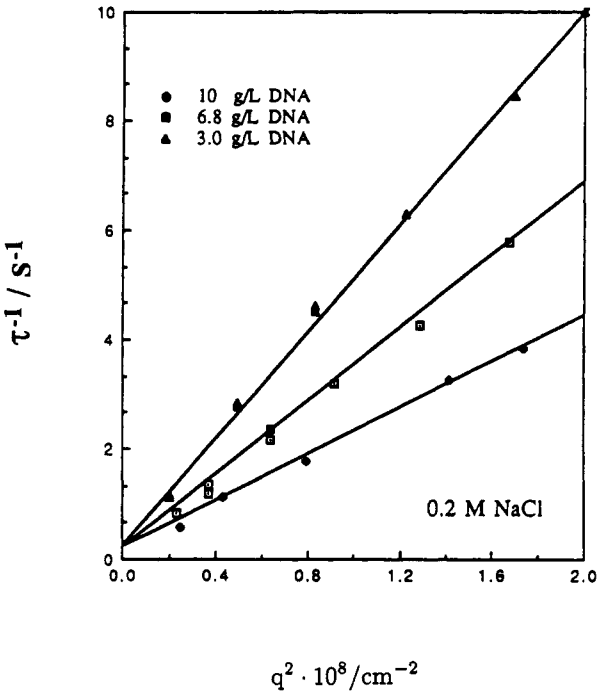


**Figure 2.** FRS signal's inverse decay time constant $\tau^{-1}$ against the square of the scattering vector $q^2$ in 0.2 M NaCl at different DNA concentrations at 20 °C. The concentrations are identified by different symbols. The self-diffusion coefficient is obtained according to eq 2; each slope corresponds to the self-diffusion coefficient at a given DNA concentration.

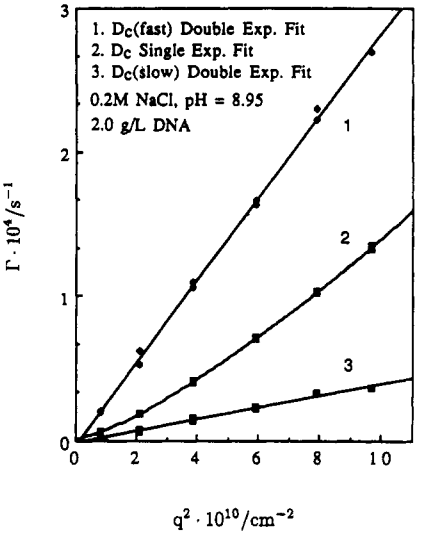


**Figure 3.** QELS autocorrelation function's decay time constant $\Gamma$ against the square of the scattering vector $q^2$ of 2 g/L of DNA in 0.2 M NaCl at 20 °C. The different fitting routines are identified by different symbols. The cooperative diffusion coefficient is obtained according to eqs 3 and 4. $D_c$(fast) and $D_c$(slow) were obtained from the slopes of line 1 and line 3, which were fit with the double-exponential function. The curved line 2 was fit with the single-exponential function.

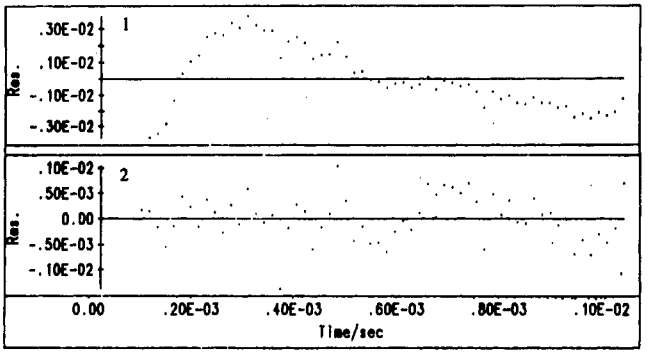


**Figure 4.** Normalized residuals from both fitting routines of the same solution as in Figure 3 at an angle of 90° by QELS. In the top portion of the figure, the oscillating (nonrandom) profile of the residuals shows a poor fit by the single-exponential function, while the random profile of the residuals in the bottom of the figure shows a good fit by the double-exponential function.

experiment was performed by using a 64-channel real-time autocorrelator (K7025; Malvern Instruments, Ltd., Malvern, Worchester, U.K.) connected to a commercial goniometer (Malvern RR103). The autocorrelation function of the scattered incident light from an argon ion laser (Lexel 75-2) at 488-nm wavelength was acquired as a function of scattering angle from 30° to 130° with a selected photomultiplier tube (ITT FW 130) operated in a photon-counting mode. The addition of a temperature-control coil to the goniometer sample holder allowed temperature regulation in the range 5–35 °C to better than ±0.2 °C. An Apple II microcomputer interfaced to the correlator provided data storage and preliminary analyses. Subsequent detailed fittings to various model functions were performed by using nonlinear regression routines on a Vax 8600 computer. The normalized intensity autocorrelation function for homodyne detection arising from a single diffusive process with the decay constant $\Gamma$ can be written as

$$g^{(2)}(t) = B + A_0 e^{-2\Gamma t} \tag{3}$$

or a double diffusive process with two decay constants as

$$g^{(2)}(t) = B + A_0(A_1 e^{-\Gamma_1 t} + A_2 e^{-\Gamma_2 t})^2 \tag{4}$$

with

$$\Gamma = Dq^2, \quad \Gamma_1 = D_1 q^2, \quad \Gamma_2 = D_2 q^2 \tag{5}$$

where $B$ is the background signal, $A_i$ ($i$ = 1, 2) is a constant, $D_i$ is the diffusion coefficient, and $q$ is the magnitude of the scattering wave vector, defined as $(4\pi n/\lambda)\sin(\theta/2)$ with $n$ being the refractive index of the medium, $\lambda$ the incident wavelength in vacuo, and $\theta$ the scattering angle.

In very low DNA concentration and high-salt concentration, quasi-elastic light scattering experiments give evidence for only one relaxation mode. In these cases, we fit experimental points by an exponential function of eq 3. In a majority of cases, however, the autocorrelation function gives strong evidence for the existence of two relaxation modes. In such a case, the double-exponential function (eq 4) was used to fit the data. The $q^2$ dependences of the inverse relaxation time for both fast and slow modes are shown in Figure 3; $\Gamma_1$(fast) and $\Gamma_2$(slow) are both found to be proportional to $q^2$. If we insist on fitting to the single-exponential model function, then the $q^2$ plot of the inverse of relaxation time becomes curved (curve 2 of Figure 3). At low scattering angles, the slope is close to the diffusion coefficient of the slow mode; at high angles the slope is close to that of the fast mode. The quality of the fit was tested by plotting the residuals against sampling time or channel number; an example of such is shown in Figure 4.

It was expected that the double-exponential fit gave small random residuals (±1 mV), indicating a good fit. Of course, the single-exponential model function gave poor fitting with oscillating (nonrandom) residuals (±3 mV). Normally, we performed two separate experiments on each solution using two different sampling times. An optimum sampling time for a given sample was selected by examining its dependence on the recovery of the base line of the relaxation process in question at one angle. Once this is done, the sampling times for the rest of the angles were chosen by maintaining the product of $q^2$ and keeping the sampling time approximately constant.

An example of the fast diffusion coefficient dependence on the sample time was shown in Figure 5. If the sample time were smaller than 0.5 μs, the average residual became quite large, indicating a wrong choice. If the sampling time were chosen to be too long, then the average residuals also became large. In such cases, the sample time of about 1 μs, a compromise between the short and long sample time, was chosen and the single-

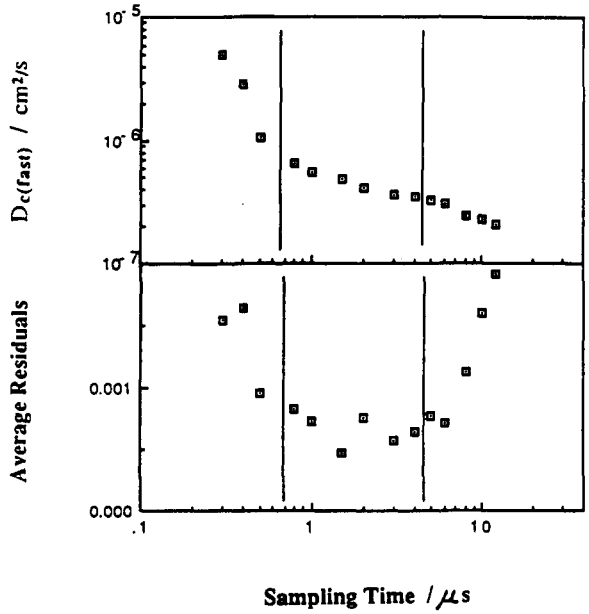


**Figure 5.** Sampling time dependence of the $D_c$(fast) and their average residuals for 3.5 g/L of DNA in 1 mM NaCl, 2.5 mM Tris, pH 8.95, 20 °C by QELS at an angle of 30°. The sampling times larger than 5 μs or smaller than 0.4 μs show large average residuals. This indicates the existence of $D_c$(fast) in the extraordinary phase. In this case, a 1-μs sampling time was chosen in our experiment.

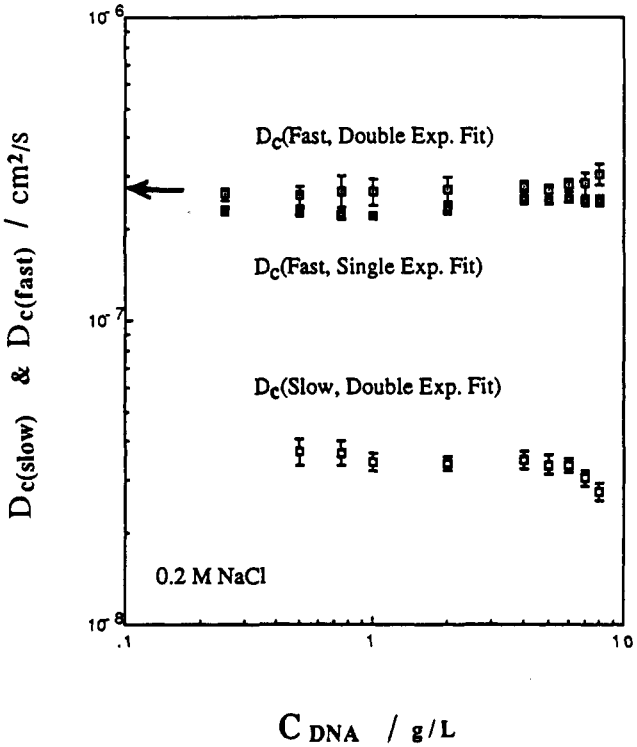


**Figure 6.** DNA concentration dependence of the cooperative diffusion coefficients in 0.2 M NaCl at 20 °C. $D_c$(fast) and $D_c$(slow) were obtained from the fit with the double-exponential function. The similar $D_c$(fast) values were obtained with the short sampling time experiment with the single-exponential function fitting routine.

exponential fit was used. The $D_c$(fast) obtained from the short sample time was very close to that obtained from double-exponential fit, which is shown in Figures 6 and 7. The $D_c$(slow) obtained from the long sample time was close to the value from the double-exponential fit. Sometimes, especially in high DNA concentrations under 1 mM NaCl condition, the intensity correlation function is clearly the sum of two exponential functions where the average decay rate values are in a ratio of approximately

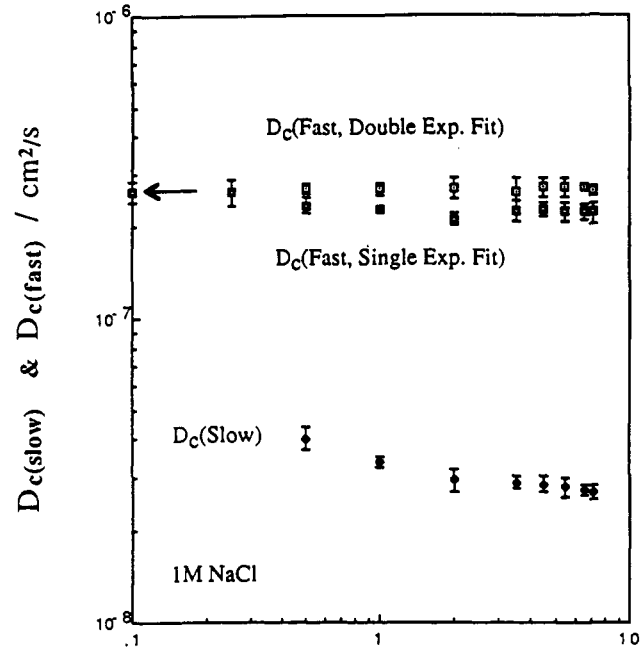


**Figure 7.** DNA concentration dependence of the cooperative diffusion coefficients in 1.0 M NaCl at 20 °C. $D_c$(fast) and $D_c$(slow) were obtained from the fit with the double-exponential function. The similar $D_c$(fast) values were obtained with the short sampling time experiment with the single-exponential function fitting routine.

100:1 or more. In such an instance, it is impossible for the autocorrelation function to cover the fast and slow modes in one experiment. Thus, two separate QELS run on each solution with different sampling times were used. In the short sampling time (0.4–6 μs) experiments, the fast diffusion coefficient was deduced to be about $10^{-6}$–$10^{-7}$ cm²/s, while in the long sampling time (10–230 μs) experiments, $D_c$(slow) ≈ $10^{-8}$ cm²/s was obtained. Generally, the scattering intensity was lower at low-salt conditions than at high-salt conditions.

## Results and Discussion

**1. Phase Boundaries of Rodlike DNA Solution.** In this paper, the contour length $L$ of our DNA fragment is 510 Å (150 bp × 3.4 Å/bp), which has been confirmed to be a rodlike chain, according to Lewis and Pecora.[24] The persistence length estimates are 500 and 1000 Å in high and low ionic strengths, respectively. Solutions of short, rodlike fragments of DNA can exist in at least four different states.[14] On the basis of Stigter's arguments,[28] the phase boundaries are estimated and collected in Table I. In this paper our concern is the concentration range, which is far below the isotropic and anisotropic transition.

**2. Diffusion in Dilute Solution.** In very dilute solutions, the diffusion coefficients depend only on the rod dimensions, solvent viscosity, and temperature. For 150 bp rodlike DNA with a length of 510 Å, the overlap concentration $C^* \approx 1/L^3 \approx 1.25$ g/L. In Figures 6–8 are displayed plots of $D_c$ vs DNA concentrations for three different salt concentrations. The salt concentration spans for three logarithmic decades, 1 mM to 1 M. The conformational invariance of the DNA fragment upon an increase of $C_s$ is to be expected and so demonstrated by constancy of $D_c$(fast) in 0.2 and 1 M NaCl. We can calculate the infinite dilution limit of the diffusion coefficient, $D_0$, with use of the length parameters of Elias and Eden[31] for DNA, a rod length $L$ = 510 Å = 150 bp × 3.4 Å/bp and diameter $d$ =

**Table I**
**Various Critical Concentrations and Diameters of 150 bp DNA at Three Ionic Conditions**

| | concentrations of DNA, g/L | | |
|---|---|---|---|
| | 0.001 M NaCl at $d$ = 529 Å[a] | 0.20 M NaCl at $d$ = 44.1 Å[a] | 1.00 M NaCl at $d$ = 29.7 Å[a] |
| $1/L^3$[b] | 1.25 | 1.25 | 1.25 |
| $1/dL^2$[b] | 1.21 | 14.5 | 21.9 |
| $2.26/dL^2$[c] | 2.73 | 32.8 | 49.5 |
| $4.25/dL^2$[d] | 5.14 | 61.6 | 93.1 |
| $5.70/dL^2$[d] | 6.89 | 82.7 | 125.0 |

[a] $d$, the diameter values at various ionic strengths, were from Stigter's calculations.[28] [b] $1/L^3 \sim 1/dL^2$ was the range of semidilute solutions of rodlike molecules.[1] [c] $2.26/dL^2$ was defined by Keep and Pecora[25] as the ordering concentration. [d] $4.25 \sim 5.70/dL^2$ was the isotropic and anisotropic transitions according to Onsager.[26]

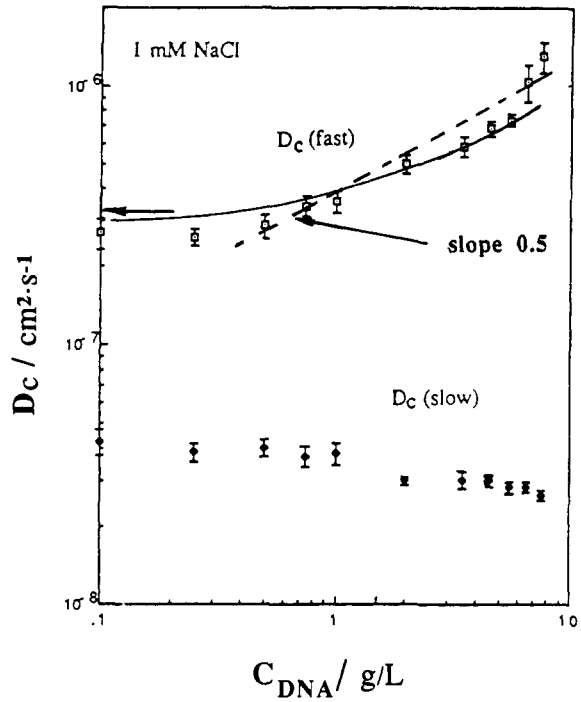


**Figure 8.** DNA concentration dependence of the cooperative diffusion coefficients in 1 mM NaCl at 20 °C. $D_c$(fast) and $D_c$(slow) were obtained from the fit with the double-exponential function. The solid line was calculated from eqs A11 and A12 of ref 11. The dashed line with a slope of 0.5 was predicted from the scaling relation.

26 Å, via the Broersma formula[32]

$$D_0 = (kT/3\Pi\eta_s L)[\ln (L/d) + \gamma] \quad (6)$$

where $kT$ has the usual meaning, $\eta_s$ is solvent viscosity, and $\gamma$ is the correction factor for end effect of a hydrodynamic cylinder model.[31,33] Here we choose $\gamma = 0.33$ at $L/d \approx 20$, following the corrections to the Broersma's original $\gamma$ value by Tirado and de la Torre.[34] The calculated $D_0$ at 20 °C is $2.75 \times 10^{-7}$ cm²/s, and this is indicated by arrows on the ordinates in all three figures. Agreement is remarkable indeed. This is also in accord with the value reported by Fulmer et al.[15]

**3. Concentration Dependence of Cooperative Diffusion in 0.2 and 1 M NaCl.** In the semidilute solution ($1/L^3 < C < 1/dL^2$), Doi and Edwards' theory[1] assumed that translational diffusion perpendicular to the long rod axis is prevented, while there would be no effect on diffusion parallel to the axis. This assumption leads to the conclusion that the translational diffusion coefficient measured by dynamic light scattering in the semidilute region should decrease to half its infinite dilution value. Such has been confirmed by Jamieson et al.[37] and Zero and Pecora[36] and not by Russo et al.[35] and Keep and Pecora.[25]

With the DNA concentration range of 0.1–10 g/L studied here for two salt conditions of 0.2 and 1 M NaCl, we are roughly in the semidilute solution range defined by Doi and Edwards[1] since $L$ = 510 Å and $d$ = 30 and 44 Å in 0.2 and 1 M NaCl solution, respectively, give $C^* \approx 1/L^3 \approx$ 1.25 g/L and $C^* \approx 1/dL^2 \approx$ 14 and 22 g/L for the two salt conditions. QELS autocorrelation functions were analyzed in terms of a double-exponential function (eq 4). The three significant parameters are the fast diffusion coefficient $D_c$(fast), the slow diffusion coefficient $D_c$(slow), and the ratio of the amplitudes of the two exponentials. The parameters were obtained as functions of the scattering angle and polymer concentration. $D_c$(fast) and $D_c$(slow) are plotted as functions of DNA concentration in double-logarithmic scales in 0.2 and 1 M NaCl solutions in Figures 6 and 7, respectively. The $D_c$(fast) is invariant with the concentration while $D_c$(slow) decreases slightly with the concentration. Two different analysis methods give rise to slightly different $D_c$(fast) values. If very short sampling times (0.4–0.6 μs) were used to follow the fast mode and the single-exponential fit was tried, the $D_c$(fast) almost recovered the values obtained from the double-exponential fit, but slightly lower values indicate finite contaminations of the slow mode in the analysis, and the results are shown in Figures 6 and 7. We defer for the moment, discussing the slow diffusion coefficients. We note that the predicted decrease to half of its infinite dilution diffusion coefficient at high concentration was not observed. As alluded to earlier, this is similar to the results reported by Zero and Pecora[36] in the case of poly(benzyl L-glutamate) (PBLG) in ethylene dichloride.

Turning to amplitude ratio (data not shown), that of the slow mode to the fast mode, it is seen to increase with the concentration and to decrease with the scattering angles in both 0.2 and 1.0 M NaCl solutions. At about $C^* \approx 1.25$ g/L, this amplitude ratio jumps slightly, indicating the crossing ("caging") of DNA rods. We should further note that the slow mode appears to be dominant only at high concentrations and low angles, whereas in most of the DNA concentration range we have examined in high-salt concentration, the fast mode appears to be dominant.

**4. Concentration Dependence of Cooperative Diffusion in 1 mM NaCl.** Since $C^* \approx 1/L^3 \approx 1/dL^2 \approx 1.2$ g/L in 1 mM NaCl when $d \approx L$ (see Table I), the theory of Doi and Edwards used above in high-salt condition cannot be applied here. The situation is similar to a polyelectrolyte solution without added salt. Several scaling relations of aqueous polyelectrolytes were derived by de Gennes et al.[4] and Odijk.[5] In the semidilute solution without added salt, considerable overlap between the chains should occur, leading to a transient network with a characteristic length $\xi$, which is known to scale as

$$\xi \propto C^{-0.5} \quad (7)$$

The cooperative diffusion coefficient hence should scale as

$$D_c \propto \xi^{-1} \propto C^{0.5} \quad (8)$$

The overlap concentration $C^*$ defined by Odijk[5] can be expressed as

$$C^* \approx (16\pi l_B a L)^{-1} \quad (9)$$

where $a$ is the linear charge spacing along the chains ($a$ = 1.7 Å), $L$ the contour length of the chain, and $l_B$ the Bjerrum length, which is defined as $l_B \equiv e^2/\epsilon kT$, where $e$

is the elementary charge, $\epsilon$ is the relative permittivity of the water, and $kT$ has the usual meaning. The calculated $C^* = 1.8$ g/L, which is very close to 1.2 g/L of DNA calculated from $C^* \approx 1/L^3 \approx 1/dL^2$ in 1 mM NaCl solution. From these estimates, the overlap concentration $C^*$ in 1 mM NaCl is safely estimated to lie in the range of 1.2–1.8 g/mL.

The concentration dependence of $D_c$(fast) and $D_c$(slow) in 1 mM NaCl solution is shown in Figure 8. The DNA concentration was varied from 0.1 to 10 g/L, which covers the dilute and semidilute solution. For the two lowest concentrations, $D_c$(fast) was independent of the concentration, which is the result predicted by eq 6. At about the overlap concentration, $D_c$(fast) increases with the concentration while $D_c$(slow) decreases slightly. The whole profile was very similar to that of sodium poly(styrenesulfonate) and sodium poly(methacrylate) in low-salt conditions.[38,39] To compare our data with the theoretical predictions quantitatively, the slope (0.5 from eq 8) predicted by de Gennes et al.[4] and Odijk[5] is drawn as a dashed line in the figure. It is apparent that the curvature in the data profile is completely missed by this simple exponent. Parenthetically, similar slopes were observed with synthetic polyelectrolytes in low-salt conditions in our laboratory.[38,39] Therefore, the dynamics of DNA rodlike fragments in semidilute solution may be said to be like that of another polyelectrolyte in low-salt conditions.

Schmitz and Lu[17] have also considered coupling of translational and rotational modes for rigid rods in congested solutions as an explanation for the extraordinary diffusion regime. According to Bloomfield,[14] the model of the coupled translation–rotation modes can be ruled out for the 150 bp DNA molecules because they are too short.

The small ion–polyion diffusive modes coupling model was proposed by Lin et al.[12] In this model the fast mode reflects the coupling of small ions with isolated polyions. With use of the model (eqs A11 and A12 of ref 12), we calculate $D_c$ as a function of the concentration with the diffusion coefficients of NaCl and DNA as $1.52 \times 10^{-5}$ and $2.75 \times 10^{-7}$ cm$^2$/s, respectively, in 1 mM NaCl. The calculated concentration dependence profile of $D_c$, drawn as a solid curve, is in good agreement with the experimental data, as shown in Figure 8. However, the effective charge number ($Z = 9$) chosen to fit the data is 9, which is much smaller than the $Z$ value of 71.5 ($=150 \times 2 \times 1.7/7.13$) deduced from Manning's condensation model, which may already be an underestimate of $Z$, whereas the structural $Z$ value is 300. We are thus compelled to conclude that the profile of $D_c$ with concentration is well reproduced, provided we pick an unusually small value, hence perhaps a physically unreasonable one, for the effective charge number $Z$; the basis of the discrepancy is obscure though this is commonly observed with other systems as well.

Turning to the relative amplitude data, Figure 9 gives the variations of the ratio of the amplitude of the slow mode to that of the fast mode with respect to the DNA concentration at different scattering angles in 1 mM NaCl. At about the overlap concentration $C^* \approx 1.0$–$2.0$ g/L, this amplitude ratio jumps dramatically, which appears to be consistent with our estimate of $C^*$ from the three different ways. The ratio is less than 1 at DNA concentrations below 1 g/L, indicating that the fast component is the dominant one in the dilute region. The slow mode increases as the concentration increases (and $q^{-1}$ increases) above the overlap concentration. The big jump observed in the concentration profile may be the "ordinary to extraordinary" phase transition observed by Fulmer et al.[15] and Schmitz and Lu[17] in their salt concentration profiles. The transition occurred at a concentration that is below the isotropic–anisotropic transition estimated by Stigter[29] while the ordinary–extraordinary transition of polylysine solution occurred at a greater polymer concentration than the isotropic–anisotropic transition.[29] The reason for this discrepancy is not clear, although one obvious difference is that DNA is a rodlike chain while polylysine is semiflexible. We will return to a detailed discussion of the slow mode.

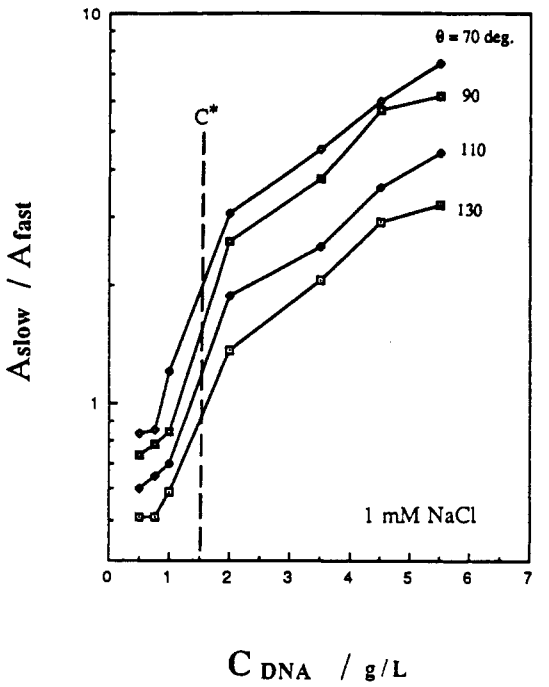


**Figure 9.** Amplitude ratio (slow/fast) from the double-exponential function fit plotted as a function of DNA concentration at four different angles. The experimental conditions were the same as those in Figure 8.

**5. Self-Diffusion.** The self-diffusion behavior is different from the cooperative diffusion behavior, as outlined to this point. Only one relaxation mode was observed, and the decay profiles can be fitted with a single-exponential function. The self-diffusion coefficient $D_s$ is plotted as a function of the DNA concentration at three different NaCl solutions in Figure 10. $D_s$ has a very weak DNA concentration dependence below the overlap concentration. Above the overlap concentration, $D_s$ decreases as the concentration increases in each salt concentration, as would be expected. On the basis of the scaling relations of de Gennes et al.[4] and Odijk[5] without added salt, Wang et al.[38] derived an exponent of −0.5 for the self-diffusion coefficient, which is drawn in Figure 10 for comparison. The scaling prediction and the experimental results are qualitatively in agreement. It seems that smaller self-diffusion coefficients below the overlap concentration might be explained by the augmented diameter of the DNA rods ($d$ = 529 Å in 1 mM NaCl) in low-salt concentration, on top of the high DNA concentrations used in our experiment. Both lead to very strong interactions among the charged rods. The augmented diameter upon lowering NaCl concentration might be used to explain the salt effect of self-diffusion coefficients qualitatively. However, we believe that further theoretical treatment is needed to account fully for the salt effect.

**6. Comments on Slow Mode.** The slow mode was observed by QELS in many polyelectrolyte systems.[7,8,10,11] It has been suggested that the slow mode reflects a repta-

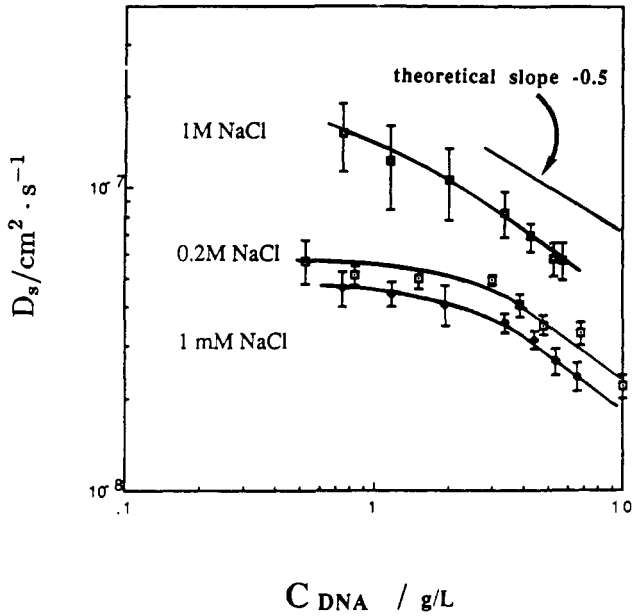


**Figure 10.** DNA concentration dependence of the self-diffusion coefficients $D_s$ in three different salt concentrations at 20 °C.

**Table II**
**EDTA Concentration Dependence of Cooperative Diffusion Coefficients[a]**

| EDTA concn, mM | $D_c$(fast) × $10^7$,[b] $cm^2/s$ | $D_c$(slow) × $10^8$,[b] $cm^2/s$ |
|---|---|---|
| 0.1 | 2.85 (±0.08) | 4.07 (±0.03) |
| 1.0 | 2.76 (±0.09) | 4.67 (±0.40) |
| 10.0 | 2.60 (±0.13) | 3.58 (±0.47) |

[a] 2.0 g/L of DNA in 0.2 M NaCl, 2.5 mM Tris, and pH = 8.95 buffer solutions. [b] These values were obtained by fitting to the double-exponential decay function.

tive diffusion process[10,11] because $D_c$(slow) decreases with increasing concentration as would be expected for self-diffusion through an increasingly congested solution. In an earlier study of 150 bp DNA solution, the slow mode was observed by QELS,[15] where once DNA concentration was fixed, the slow mode was not dependent on added salt concentration.[14] The slow mode was also observed in 350 bp DNA solution.[17] The origin of the slow mode is not clear, and more work was invited.[14]

It was reported that DNA underwent unimolecular and paucimolecular condensation into toroids in the presence of multivalent cations.[40,41] It therefore might be plausible that the slow mode is attributed to such condensation caused by contaminating multivalent cations. We hence undertook to examine concentration dependence of EDTA, an efficient chelator, on the slow mode with 2 g/L DNA in 0.2 M NaCl. The results are collected in Table II. The $D_c$(slow) was not changed as EDTA concentration was increased from 0.1 to 10 mM. To test the DNA condensation by multivalent cations, a small amount of $FeCl_3$ was added to a 0.1 g/L DNA solution under the same salt conditions, in which the slow mode was initially not observed. We found that a very slow diffusion coefficient ($\sim 10^{-9}$ $cm^2/s$) was observed upon addition of $FeCl_3$. The slow diffusion coefficient was increased immediately by a subsequent addition of EDTA. The results thus suggest that the slow mode was not caused by the contaminating multivalent cations.

Kinetics of the slow-mode appearance was examined qualitatively through the correlation function. The slow mode can be abolished by filtration through Nucleopore filters (500 Å), which is the length of the DNA fragment.

**Table III**
**Temperature Dependence of Cooperative Diffusion Coefficients[a]**

| $T$/K | $D_c$(slow)-$[T_0\eta_s(T)/T\eta_s(T_0)] \times 10^8$,[b] $cm^2/s$ | $D_c$(fast)-$[T_0\eta_s(T)/T\eta_s(T_0)] \times 10^7$,[b] $cm^2/s$ |
|---|---|---|
| 276 | 4.02 (±0.09) | 3.77 (±0.33) |
| 278.5 | 3.78 (±0.10) | 3.78 (±0.30) |
| 283 | 3.67 (±0.25) | 3.81 (±0.40) |
| 286 | 3.52 (±0.13) | 3.83 (±0.50) |
| 290 | 3.09 (±0.27) | 3.97 (±0.6) |
| 293 | 3.06 (±0.16) | 3.81 (±1.0) |

[a] 2 g/L of DNA in 1 mM NaCl, 2.5 mM Tris, pH = 8.95 buffer solution. [b] $T_0$ = 293.15 K and $\eta_0$ = 0.01 P. A double-exponential fitting routine was used. The solutions were kept at the same temperature overnight before the measurements.

No slow mode could be detected immediately after the filtration. However, a small but finite slow mode can be detected within 5 min after filtration. A rather obvious slow mode can be measured precisely within 30 min after filtration. The results are similar to the observation by Nicolai and Mandel.[6] All our experiments were done 30 min after filtration through Millipore filters (0.22 μM).

The temperature dependence of the slow mode with 2 g/L DNA in 1 mM NaCl is listed in Table III. The $D_c$(slow) was obtained after the DNA solution was kept in the same temperature overnight in order to ascertain the equilibrium conditions. The results show that $D_c$(slow) was not changed if the sample was kept longer than overnight. The maximum temperature was 20 °C to be sure that the sample would not denature. The temperature was varied from 3 to 20 °C and at six different temperatures. As the temperature was increased from 3 to 20 °C, the temperature–viscosity-corrected $D_c$(slow) decreased from 4.02 × $10^{-8}$ to 3.06 × $10^{-8}$ $cm^2/s$. The slow mode slows down with increasing temperature. This is contrary to the common trend of the temperature dependence of a diffusion process. The same trend was observed in a rotational correlational time vs temperature profile by Mandelkern et al.[41] in the same temperature range. They account for their data by a "bundle formation". It was said[41] that enthalpy change ($\Delta H$) was positive for the process, and the process must be entropy driven. It might be speculated that the slow mode is different from a diffusion process. Nevertheless, $D_c$(slow) has the $q^2$ dependence expected for the spatial component of a diffusion process. We should mention that the observed $D_c$(fast) seems to show the temperature dependence of a real diffusion process, which was also observed in the case of sulfonated polystyrene in low-salt conditions.[9]

We now turn to the question of whether the slow mode is a self-diffusion process that can be made relevant to the reptation mechanism, as has been mentioned above. To answer this question, the cooperative diffusion data in Figures 7 and 8 as well as the self-diffusion data in Figure 10, in 1 mM and 1 M NaCl, are plotted as a function of the DNA concentrations in Figure 11. For clarity, the dashed curves are drawn over the $D_s$ data to distinguish them from $D_c$(slow) data, and the corresponding data in 0.2 M NaCl are not plotted. As the DNA concentration increases, $D_c$(fast) increases while $D_c$(slow) and $D_s$ decrease. The self-diffusion curve is in between the $D_c$(fast) and $D_c$(slow). The concentration profiles of both diffusion coefficients are very similar to that of synthetic polyelectrolytes in low-salt conditions.[38,39] $D_c$(fast) and $D_s$ have a substantial salt effect while $D_c$(slow) has no salt dependence, which is also consistent with the observation of the slow mode by Fulmer et al.[15] *Clearly, the slow mode is not the self-diffusion process.* Not only are their

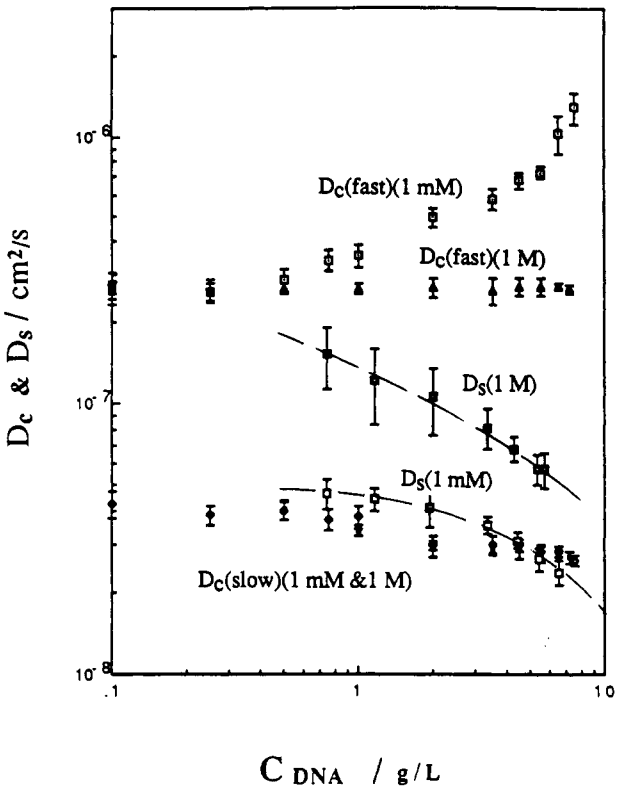


**Figure 11.** DNA concentration dependence of the self-diffusion coefficients, $D_s$, and the cooperative diffusion coefficients, $D_c$(fast) and $D_c$(slow), in 1 mM and 1 M NaCl at 20 °C. The cooperative diffusion coefficients are reproduced from Figures 7 and 8. The self-diffusion coefficients are reproduced from Figure 10 and dashed curves drawn over the data for clarity. Both diffusion coefficients were obtained at the identical conditions.

values different but they also have different salt dependences. The slow mode also has a temperature dependence different from that of a diffusion process; it does not scale with $T/\eta_s$. Thus, its origin is still obscure. We conclude only that the slow mode is not ascribed to the self-diffusion process.

The slow mode is proposed to be due to association and dissociation processes of these charged rods through the mobile, loosely associated small ions. More precisely, the slow mode is the interdiffusion mode, which is the relative motion of the single chain from one temporal cluster to another nearby cluster.[43,44] The interdiffusion idea would explain that $D_c$(slow) is smaller than $D_s$ in moderate polymer concentrations. $D_s$ might be smaller than $D_c$(slow) in the very high polymer concentrations. This interdiffusion model, at least qualitatively, can explain all experimental results in those systems where the $D_s$ and $D_c$(slow) were measured.[7,8,38,39] In DNA solutions with the salt concentration varying from 1 mM to 0.2 M NaCl, the slow mode becomes progressively less prominent, as surmised from the amplitude data shown in Figure 9. Essentially, the salt can screen the charges on the rods and reduces the association and dissociation processes or the interdiffusion process. The self-diffusion of the rods does not appear to be coupled with the process. The association and dissociation process, of course, is not sensitive to either DNA concentrations or salt concentrations while the self-diffusion process is very sensitive to both effects. Although the self-diffusion coefficients are almost 1 order of magnitude higher than the $D_c$(slow) in 1 M NaCl, $D_s$ is even smaller than $D_c$(slow) at high DNA concentrations in 1 mM. The lifetime of the slow mode is longer than 1–120 μs (sampling time in QELS experiments) but shorter than 500–2000 ms (sweeping time in FRS experiments). QELS probes the density fluctuation of the solution, so this technique is very sensitive to the association and dissociation processes in short scale ($d$ = 690–200 nm). The FRS probes self-diffusion, which traces single-chain motion in the congested solution in large length scales ($d$ = 12–2.3 μm), so that FRS is seemingly insensitive to the presence of the slow mode in long time and large length scales. The small ion-coupled model of Lin et al.[12] was used to explain discrepancy of experimental results between QELS and fluorescence photobleaching recovery in polylysine solution by Schmitz et al.[42] In this paper the slow mode is a result of sharing small ions between several polyions. These temporal aggregates are stabilized by a delicate balance between the attractive force arising from the fluctuating dipole field generated from the sharing of small ions by several polyions and the repulsive forces due to direct electrostatic interactions between charged polyions. The idea is not yet fully formulated in our opinion and cannot be tested by experiment quantitatively. Nevertheless, the idea of temporal aggregates is an attractive one.

## Conclusions

Although it might be premature to claim that the scaling predictions of de Gennes et al.[4] and Odijk[5] as well as the small ion–polyions coupled theory by Lin et al.[12] are all fully borne out by our experiments with rodlike DNA solutions, our results are consistent with these predictions, at least qualitatively. In high-salt conditions, the concentration independence of the $D_c$(fast) is consistent with the prediction of the Doi and Edwards' theory,[1] whereas the predicted half of that in the infinite dilution limit was not borne out. From the coupled diffusive modes theory, the calculated values can mimic the experimental data in low-salt conditions. The DNA concentration dependence of $D_c$(fast) and $D_s$ might be explained in terms of the scaling relations of the interacting rods by de Gennes et al.[4] and Odijk[5] in low-salt conditions. The slow mode is found not to be the self-diffusion process.

**Acknowledgment.** This work is in part supported by the Biophysics Program and Polymers Program of the National Science Foundation. We gratefully acknowledge Professor M. Thomas Record for generously making the facility of his laboratory available to us and Professors J. M. Schurr and Victor A. Bloomfield for fruitful discussions. We are also indebted to Dr. Brough Richey and Mr. Richard B. Dowd for their help with the DNA preparation and characterization.

## References and Notes

(1) Doi, M.; Edwards, S. F. *J. Chem. Soc., Faraday Trans. 2* **1978**, *74*, 560–570 and 918–932.
(2) Fixman, M. *Phys. Rev. Lett.* **1985**, *54*, 337, 55, and 2429.
(3) Doi, M.; Shmada, T.; Okano, K. *J. Chem. Phys.* **1988**, *88*, 4070–4075.
(4) de Gennes, P.-G.; Pincus, P.; Velasco, R. M.; Brochard, F. *J. Phys. (Paris)* **1976**, *37*, 1461–1473.
(5) Odijk, T. *Macromolecules* **1979**, *12*, 688–693. Odijk, T. *J. Polym. Sci., Polym. Phys. Ed.* **1977**, *15*, 477–483.
(6) Nicolai, T.; Mandel, M. *Macromolecules* **1989**, *22*, 438–444; **1989**, *22*, 2348–2356.
(7) Bloomfield, V. A. In *Dynamic Light Scattering*; Pecora, R., Ed.; Plenum Press: New York, 1985; pp 363–416.
(8) Schurr, J. M.; Schmitz, K. S. *Ann. Rev. Phys. Chem.* **1986**, *37*, 271–305.
(9) Grüner, F.; Lehmann, W. P.; Fahlbusch, H.; Weber, R. *J. Phys. A: Math. Gen.* **1981**, *18*, L307–313.
(10) Koene, R. S.; Mandel, M. *Macromolecules* **1983**, *16*, 973–978.

(11) Drifford, M.; Dalbiez, J. P. *J. Phys. Lett. (Paris)* **1985**, *46*, L311–319.
(12) Lin, S. C.; Lee, W. I.; Schurr, J. M. *Biopolymers* **1978**, *17*, 1041–1064.
(13) Wang, L.; Yu, H. *Macromolecules* **1988**, *21*, 3498–3501.
(14) Bloomfield, V. A. In *Reversible Polymeric Gels and Related Systems*; Russo, P. S., Ed.; American Chemical Society: Washington, DC, 1987; pp 199–210.
(15) Fulmer, A. W.; Benbasat, J. A.; Bloomfield, V. A. *Biopolymers* **1981**, *20*, 1147–59.
(16) Fried, M. G.; Bloomfield, V. A. *Biopolymers* **1984**, *23*, 2141–55.
(17) Schmitz, K. S.; Lu, M. *Biopolymers* **1984**, *23*, 797–808.
(18) Shindo, H.; McGhee, J. D.; Cohen, J. S. *Biopolymers* **1980**, *19*, 523–537.
(19) Forster, A. C.; McInnes, J. L.; Skingle, D. C.; Symons, R. H. *Nucleic Acids Res.* **1985**, *13*, 745–761.
(20) Kim, H.; Chang, T.; Yohanan, J. M.; Wang, L.; Yu, H. *Macromolecules* **1986**, *19*, 2373.
(21) Leger, L.; Hervet, H.; Rondelez, F. *Macromolecules* **1984**, *17*, 782.
(22) Salcedo, J. R.; Siegman, A. E.; Dlott, D. D.; Fayer, M. D. *Phys. Rev. Lett.* **1978**, *41*, 131.
(23) Amis, E. J.; Janmey, P. A.; Ferry, J. D.; Yu, H. *Macromolecules* **1983**, *16*, 441–446.
(24) Lewis, R. J.; Pecora, R. *Macromolecules* **1986**, *19*, 2074–75.
(25) Keep, G. T.; Pecora, R. *Macromolecules* **1988**, *21*, 817–829.
(26) Onsager, L. *Ann. N.Y. Acad. Sci.* **1949**, *51*, 627–659.
(27) Stigter, D. *Biopolymers* **1977**, *16*, 1435–1448.
(28) Stigter, D. *Macromolecules* **1985**, *18*, 1619–1627.
(29) Stigter, D. *Biopolymers* **1979**, *18*, 3125–3127.
(30) Rill, R. *Proc. Natl. Acad. Sci. U.S.A.* **1986**, *83*, 342–346.
(31) Elias, J. G.; Eden, D. *Biopolymers* **1981**, *20*, 2369–2380.
(32) Broersma, S. *J. Chem. Phys.* **1960**, *32*, 1626–1631 and 1632–1635.
(33) Yamakawa, H.; Tanaka, G. *J. Chem. Phys.* **1972**, *57*, 1537–1542.
(34) Tirado, M. M.; de la Torre, G. *J. Chem. Phys.* **1979**, *71*, 2581–2587.
(35) Russo, P. S.; Langley, K.; Karasz, F. E. *J. Chem. Phys.* **1984**, *80*, 5312–5325.
(36) Zero, K. M.; Pecora, R. *Macromolecules* **1982**, *15*, 87–93.
(37) Jamieson, A.; Southwick, J.; Blackwell, J. *J. Polym. Sci., Polym. Phys. Ed.* **1982**, *20*, 1531.
(38) Wang, L.; Kim, S.; Shang, L.; Yu, H., to be published.
(39) Austin, M. E.; Hofer, M.; Yu, H., to be published.
(40) Wilson, R. W.; Bloomfield, V. A. *Biochemistry* **1979**, *18*, 2192–96.
(41) Mandelkern, M.; Dattagupta, N.; Crothers, D. M. *Proc. Natl. Acad. Sci. U.S.A.* **1981**, *78*, 4294–4298.
(42) Schmitz, K. S.; Lu, M.; Singh, N.; Ramsay, D. J. *Biopolymers* **1984**, *23*, 1637–46.
(43) Wang, L.; Bloomfield, V. A., unpublished.
(44) Benmouna, M.; Benoit, H.; Duval, M.; Akcasu, A. Z. *Macromolecules* **1987**, *20*, 1107–1112. Borsali, R.; Duval, M.; Benmouna, M. *Polymer* **1989**, *30*, 610–614.

**Registry No.** 4-Fluoro-3-nitrophenyl azide, 28166-06-5; *N*-(3-aminopropyl)-*N*-methyl-1,3-propanediamine, 105-83-9; 4-(*N*,*N*-dimethylamino)azobenzene 4′-isothiocyanate, 7612-98-8; 1,4-bis(3-aminopropyl)piperazine, 7209-38-3; *N*-(3-aminopropyl)-*N*′-(4-azido-2-nitrophenyl)-*N*-methyl-1,3-propanediamine, 96087-44-4; *N*-[3-[[3-[(4-azido-2-nitrophenyl)amino]propyl]methylamino]propyl]-*N*′-[4-[[4-(dimethylamino)phenyl]azo]phenyl]thiourea, 132673-90-6.